Korean J. Chem. Eng., 35(9), 1878-1888 (2018)
DOI: 10.1007/s11814-018-0091-z

pISSN: 0256-1115
eISSN: 1975-7220

Analysis of molar flux and current density in the electrodialytic separation of sulfuric acid from spent liquor using an anion exchange membrane

Beena Sheth* **and Kaushik Nath****,†**

*Department of Chemical Engineering, Viswakarma Government Engineering College, Chandkheda, 382424, Gujarat, India
**Department of Chemical Engineering, G. H. Patel College of Engineering & Technology,
Vallabh Vidyanagar, 388120, Gujarat, India
(*Received 26 January 2018 • accepted 4 June 2018*)

Abstract−Separation of sulfuric acid from a dilute solution involved a plate and frame type electrodialysis unit using a commercial anion exchange membrane. Experiments were conducted in batch with catholyte concentrations ranging from 1 to 5 wt%. Effect of applied current density, initial catholyte concentration and initial concentration difference of catholyte and anolyte on the molar flux was studied extensively. The maximum molar flux was estimated to be 10.52×10^{-8} mol $cm^{-2}s^{-1}$ at 4.45 wt% catholyte concentration and applied current density of 30 mA cm^{-2}. Current efficiencies were observed to be 75 to 85% at lower current density, which rose to more than 100% at 20 and 30 mA cm^{-2}, at equal initial concentration of catholyte and anolyte. Diffusive flux and flux due to membrane potential contributed very less compared to total flux in presence of applied electric current. An equation was developed to predict the practical molar fluxes, which fitted satisfactorily with minor standard deviation. Pristine and used membrane specimens were characterized using Fourier transform infrared spectroscopy (FTIR) and scanning electron microscopy (SEM).

Keywords: Sulfuric Acid, Electrodialysis, Current Density, Molar Flux, Current Efficiency, Catholyte Concentration

INTRODUCTION

Spent pickle liquor, more commonly termed as spent liquor, is traditionally generated from the digestion or extraction of ores with inorganic acids in metallurgical units. The liquor invariably contains residual acid and metal salts of the pickling acid. Amongst a number of metal finishing units, the iron and steel industries in particular, are significant contributors of such waste streams where hydrochloric and sulfuric acids are used as principal acids and the resulting metal salts are ferrous chloride and ferrous sulfate, respectively [1]. Disposal of spent pickle liquor is of great public concern in view of stringent environmental regulation as the liquor containing 5-10% of free acid is considered to be unsafe following EPA hazardous waste list (EPA). Conventional reclamation of the spent liquor includes processes like neutralization-precipitation [2], refrigerated crystallization [3], electrolytic precipitation-deposition [4], ion exchange [5], and relatively older methods of solvent extraction [6,7]. Despite being old, none of these processes have achieved widespread acceptance due to the cumbersome equipment required, the quantities of treating chemicals, including significant amount of makeup fresh acid consumed and low cost-benefit ratio.

Electrodialysis (ED), on the other hand, holds much promise in the treatment of acid effluents from industry. It is an electromembrane process in which ions are transported through a permselective ion exchange membrane from one solution to another under the influence of an electrical potential gradient. Electrical charges on the ions enable them to be driven through the membranes. Anions are able to permeate through anion-selective membranes, but are blocked by the cation-selective ones. The opposite occurs with cations. As a result, two different solutions are produced inside the stack: one more dilute (the diluate), and the other more concentrated (the concentrate) than the feed solution [8]. Rodrigues et al. [9] reported the potential of chromating-bath rinse water treatment by electro-dialysis, whereby optimization of waste reduction and reuse of water and chemical products could be achieved. Electro-dialysis of aqueous $CuSO_4$-H_2SO_4 based solution with metallic impurities was carried out using two lab-scale electro-dialysis (EH) cells [10]. Winniewski et al. [11] studied the acid and base purification via bipolar electrodialysis. In another study, recovery of sulfuric acid from acid mine drainage was achieved by means of a three compartment ED cell with substantial increase in acid concentration and simultaneous removal of Fe(III) ions [12]. The transport characteristics of trivalent metals Cr(III) and Fe(III)) through cation-exchange membranes with mono- and divalent ions present in solutions of sulfate salts of multivalent metals under varying electrical field were also compared [13]. ED was found suitable for recovering water from acid mine drainage generated from coal mining, with contaminant removal efficiencies reaching as high as 97% [14]. Jaroszek et al. [15] used ED to concentrate sulfuric acid by using five different types of anion exchange membranes and determined membrane susceptibility to back diffusion.

Despite several works cited on the ED process in the separation and purification of aqueous waste streams, its applicability in the recovery of spent acids from waste liquor, in particular is a less focused area of research. Moreover, its rigorous parametric evaluation by analyzing the concentration polarization of the system, the

†To whom correspondence should be addressed.
E-mail: kaushiknath@gcet.ac.in, kaushiknath2003@yahoo.co.in

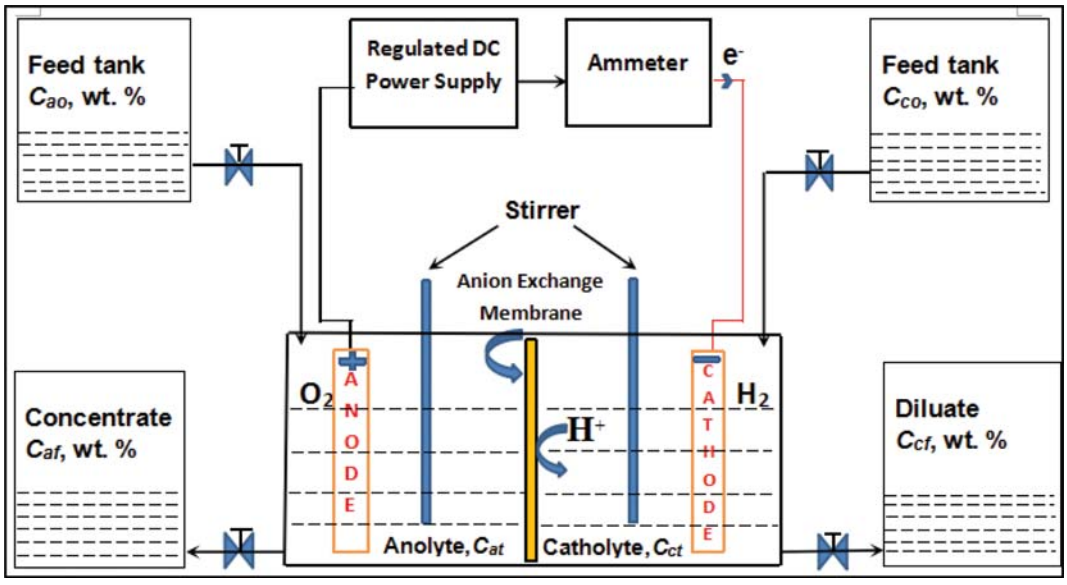

Fig. 1. Schematic representation of experimental set up used in present study.

limiting current, and flux improvement strategy for the overall recovery of acid constitutes important areas of process development. The rationale of undertaking the work stems from the need for effective treatment of dilute sulfuric acid laden wastewater. Such dilute acid streams could be concentrated initially by ED followed by any conventional techniques such as evaporation, thereby reducing the heat load on the evaporation. Energy required to increase the concentration of dilute sulfuric acid by ED can be thought to be very much lower than the same for evaporation. Supplementation of evaporation with ED cannot only be considered as a synergic combination, but also an energy efficient process. Keeping this in mind, we explored the amenability of a commercial ion exchange membrane in the ED process for improving the efficiency of recovery of sulfuric acid from spent liquors. Being hazardous and affecting living and non-living environment, it is extremely important to reduce the concentration of sulfuric acid from its solution before discharge, and acid recovered can be recycled or reused. The objectives of the present work encompass the analysis of molar flux and current density in the electrodialytic separation of sulfuric acid from dilute solution using an anion exchange membrane. Variation of concentration with time for different applied current densities and initial catholyte and anolyte concentrations were also evaluated. In addition, a model equation was developed to predict the molar fluxes during electrodialysis and to fit the experimental data.

MATERIALS AND METHODS

1. Chemicals and Membrane

All the chemicals used in the present study were of analytical grade (AR) supplied by Finar Ltd. (Mumbai, India) and were used as received without further purification. Stock solutions were prepared with deionized water, having a conductivity of 20 μS cm^{-1}, produced from a reverse osmosis system. An anion exchange Selemion AAV membrane (produced by Asahi Glass) supplied by AGC Engineering Company Limited., Chiba, Japan was used in the experiment. It is a special purpose membrane with low proton leakage having transport number for hydrogen ion very small suitable for the transport of sulfate as counter ions. The membrane has a thickness of 120 μm and effective area 49.5 cm^2. Burst strength of the membrane is 300 kPa. Allowable maximum operating temperature is 40 °C. Prior to its use in the ED cell, the membrane was soaked in water and the feed solution for more than 24 h.

2. Experimental Set-up and Operating Conditions

The experimental set-up for the ED process is schematically represented in Fig. 1. The set-up consisted of two-compartment cell having similar volume on both the side and partitioned by AAV membrane with effective area of 49.5 cm^2. Graphite anode and cathode electrodes were used with total surface area 55 cm^2. A constant current was supplied in the range from 100 mA to 2,000 mA for few min by controlling the variation in voltage. Experiments were conducted for different anolyte and catholyte concentrations and which were measured at regular interval by conductivity analysis and titrimetrically using 0.1 N NaOH solutions. Variation of volume in either compartment was found to be negligible except for a few cases while operated at high voltage. Operating time was different for different experimental runs ranging from a few min to maximum 6 h. However, for flux calculation, time was taken constant and considered initial 150 min for all experiments. Frequent stirring was provided on both the compartments to maintain the homogeneity of the solution during the experiment. Current and voltage were supplied and regulated by AC to DC converter. Dilute sulfuric acid feed solution was prepared in laboratory having different concentrations ranging from 1 to 5 wt% of concentrated sulfuric acid. Each experiment was started with some residual acid present initially in anolyte to reduce the resistance provided by distilled water.

3. Measurement of Conductivity

Concentration of electrolyte was measured by measuring conductivity of solution, using a Chemiline digital conductivity meter CL 220 manufactured by Aqua Mart, Kolkata, India having 0 to

200 mS conductivity range with measuring accuracy of 1% of full scale in all the ranges.

4. Determination of Total Flux and Current Efficiency

Taking into consideration the major variables affecting the ionic flux through the membrane, total flux of sulfate ions from catholyte to anolyte through an anion exchange membrane can be given by Eq. (1)

$$J_{total}=f(C_{co}, C_{ao}, \mu, \emptyset) \quad (1)$$

In the present study, since the feed was dilute sulfuric acid solution, viscosity for the same could be assumed to be constant with negligible contribution to flux variation. Accordingly Eq. (1) reduces to

$$J_{total}=f(C_{co}, C_{ao}, \emptyset) \quad (2)$$

In ED process the total flux is the contribution of three different types of fluxes. The flux of anions crossing the membrane results from two driving forces: the electrical potential difference and the concentration difference. Assuming unidirectional flow [16], flux due to motion/velocity of fluids (J_u); natural diffusion based on concentration gradient (J_D), migration of ions based on membrane electric potential ($J_\emptyset$) and flux due to applied electric potential ($J_{\emptyset a}$). So the total flux can be represented as

$$J_{total}=J_u+J_D+J_\emptyset+J_{\emptyset a} \quad (3)$$

In the present system, flux of sulfate ions was studied and all the terminologies were used for the molar flux of sulfate ions only. Furthermore, it was assumed that the sulfuric acid is completely dissociated inside the membrane phase [17]. In the given process, the velocity component is zero, i.e. flux contribution due to motion of fluid is zero. Therefore,

$$J_u=0 \quad (4)$$

Based on velocity component zero, Eq. (4) reduces to,

$$J_{total}=J_D+J_\emptyset+J_{\emptyset a} \quad (5)$$

The contribution of unidirectional diffusive flux was calculated for different initial anolyte and catholyte concentration.

4-1. Flux Due to Diffusion of Ions Across the Membrane (J_D)

Diffusive flux [18] through the membrane can be represented by Eq. (6)

$$J_D=-D\frac{dC_t}{dx} \quad (6)$$

$$J_D]_{t=0}=-D\frac{(C_{ao}-C_{co})}{dx} \quad (7)$$

Eq. (7) represents the diffusive flux at t=0 when $C_{ct}=C_{co}$ and $C_{at}=C_{ao}$, initially when the separation starts. Eq. (6) gives the diffusive flux at particular instant of time. The value of D is 5.1×10^{-7} mol cm^{-2} for AAV is membrane [18].

4-2. Flux Due to Membrane Electric Potential Generated ($J_\emptyset$)

According to the classical Nernst-Planck electro-diffusion law [16,17,19], flux through membrane based on concentration gradient is given by Eq. (8),

$$J_\emptyset=-mzC_{co}\frac{dV_m}{dx} \quad (8)$$

where m is the mobility of ions in the liquid and V_m is the membrane potential. The relation between mobility of ions and diffusivity is

$$m=DF/RT \quad (9)$$

$$J_\emptyset=\frac{-DzFC_{co}\left(\frac{dV_m}{dx}\right)}{RT} \quad (10)$$

Eq. (10) gives the molar flux of sulfate ions through the membrane, based on the Nernst potential generated ideally in absence of external electric field.

where V_m is calculated using Eq. (11),

$$V_m=\frac{RT\ln\left(\frac{C_{ao}}{C_{co}}\right)}{Fz} \quad (11)$$

Combining Eqs. (6) to (10), the contribution of flux due to concentration gradient and the Nernst membrane potential generated can be represented by Eq. (12)

$$J_D+J_\emptyset=-D\frac{dC_t}{dx}+\frac{-DzFC_{co}\left(\frac{dV_m}{dx}\right)}{RT} \quad (12)$$

Eq. (12) can be rearranged for constant membrane thickness x, ($J_D+J_\emptyset$) values calculated using Eq. (13)

$$J_D+J_\emptyset=-DdC_t+\frac{-DzFC_{co}V_m}{RT} \quad (13)$$

When ED is carried out batchwise in the presence of an applied electric field, by attaching battery with the anode and cathode, the contributions of the diffusive flux and the Nernst potential flux will be different. These can be calculated on the basis of average values of concentration with time, for interval of 30 min each for entire experimental run time. Eq. (13) was used to calculate the flux values J_D and $J_\emptyset$ in presence of current.

In most of the cases, except at lower applied current values, either in presence or in absence of current the flux can be calculated based on concentration gradient or the Nernst membrane potential generated. Diffusion flux in addition to the Nernst potential flux has very little contribution to the total flux because of applied electric field. Thus, under the influence of electric field, Eq. (3) can be approximated as,

$$J_{total}\approx J_{\emptyset a} \quad (14)$$

Current efficiency is the actual current utilized by the ions for their movement from cathode to anode per current supplied [20]. Current efficiency was calculated using Eq. (15),

$$CE=\frac{z(C_{cf}-C_{co})V_lF}{It} \quad (15)$$

5. Practical Flux Calculation (J_p)

Practical flux, which is calculated using Eq. (16), is expressed as the net flux of sulfate ions crossing the membrane and is directly related to the variation in amount of sulfuric acid in either catholyte or anolyte,

$$Jp = \frac{dC_c}{dt} \quad (16)$$

Eq. (16) can be integrated over the experimental time interval, to calculate total flux,

$$Jp = \int_0^t \frac{dC_c}{dt} \quad (17)$$

Eq. (17) can be divided by membrane area A to calculate total molar flux per unit area of membrane practically in mol cm^{-2} s^{-1} for actual volume of the system.

6. Flux Calculation Based on a Model Equation (J_m)

It was observed that the total flux was not only the contribution of diffusive and electrochemical flux, but there was a definite effect of applied current density on it as well. According to the Nernst-Planck equation, when there is no concentration difference, no membrane potential gradient is generated: V_m=0. Hence, net fluxes are also considered zero. As applied current density was increased, there was an increase in molar flux for same concentration values of anolyte and catholyte. Therefore, the effect of applied current density (I_c) must be taken into account. Considering this effect, Eq. (18) was proposed to calculate molar flux.

$$J_m = A + aI_c^b + cC_{co}^d \quad (18)$$

Eq. (18) was used when $C_{co} \neq C_{ao}$. Diffusion flux was assumed to be negligible in flux calculation as their effect was very less in the presence of higher applied currents. All the constants and coefficients of Eq. (18) were calculated using SOLVER analysis tool in excel.

7. FTIR Analysis

The presence of organic functional groups on the membrane surface was analyzed by Fourier transform infrared spectroscopy (Perkin Elmer Spectrum GX) using a wave number range of 400-4,000 cm^{-1} at a resolution of 4.0 cm^{-1} with an acquisition time of 1 min. Wet samples were prepared by thoroughly cleaning pristine membrane coupons with deionized water and soaking them in a water bath for 24 h. The dried samples were sandwiched into a special folder and fixed with transparent tape for absorption measurement. The sampling chamber was continuously purged with nitrogen gas at a flow rate of 10 mL min^{-1} to avoid signal interference from the surrounding moisture and CO_2. At least 2 replicates were obtained for every sample type without applying any baseline corrections.

8. FE SEM Analysis

The outer surface topology of the AAV membrane was investigated by field emission scanning electron microscopy (FE-SEM) using JEOLFE-SEM (JSM-6701F) at 5 kV. For cross sectional analysis, cryogenically fractured membrane samples under liquid N_2 were freeze-dried overnight and sputtered with a thin layer of platinum using JEOL JFC-1600 auto fine coater.

RESULTS AND DISCUSSION

Molar flux across the ion exchange membrane is an important index of electrodialytic separation. Although the Selemion AAV membrane used in the present study was an anion exchange membrane, minor leakage of proton was unavoidable. Ideally, at the catholyte-membrane interface, the bisulfate ion HSO_4^- dissociates into sulfate ion which crosses the membrane and a proton remains in the cathode compartment [17,19,21,22]. Present process being a batch one, catholyte and anolyte concentration, along with molar flux varied with passage of time. Effects of various parameters on molar flux are discussed in the following sections.

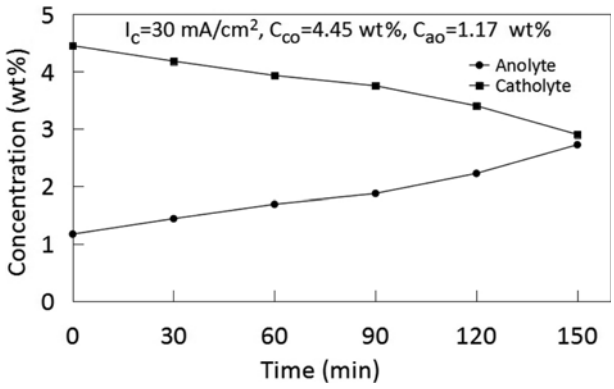

Fig. 2. Catholyte and anolyte concentration profile under electrodialytic conditions.

1. Molar Fluxes Across an Anion Exchange Membrane

Fig. 2 represents the variation of anolyte and catholye concentration with time under constant applied current density. The trend indicates that while catholyte concentration decreases with time, the anolyte concentration increases [21-25]. A close inspection of Fig. 2 reveals that catholyte concentration decreased to 2.9 wt% from an initial value of 4.45% whereas the anolyte concentration rose up to 2.72% from an initial value of 1.17% after 150 min of operation. In unsteady state batch ED process, since both the concentrations change with time, the concentration gradient could not be maintained throughout the run. Concentration gradient was also found to vary with time (data not shown).

The magnitude of various fluxes as estimated following equations in the previous section is presented in Table 1. Fluxes were calculated both in presence and in absence of current [I_c=0] as the membrane potential was generated on the bases of catholyte and anolyte concentration gradient. When no current was supplied to the system, potential developed across the membrane was calculated and shown as V_m. As Nernst membrane potential V_m is a function of concentration ratio, all V_m values are zero when anolyte and catholyte initial concentrations are same. All flux values were calculated based on average values of V_m generated naturally during each 30 min period of total experimental run as shown in Table 1. Data indicate that the contribution of diffusive flux (J_D) as well as membrane potential based flux ($J_\emptyset$) was very much less as against practical flux either in presence of applied electric current or even in its absence. It is evident from Eq. (14) that, when J_u=0, the contribution of J_D and $J_\emptyset$ in the total flux is negligible. Thus the total flux (J_{total}) is mainly the contribution of flux ($J_{\emptyset a}$) due to the applied electric field only.

Practical flux values were found to be much larger than all other flux values. Practical flux (Jp) is influenced by the applied current, whereas J_D and $J_\emptyset$ values have major influence of concentration gradient and membrane potential generated based on initial cathol-

Table 1. Various fluxes through an anion exchange membrane under electrodialysis process

Exp. Run.	I_c, mA/cm^2	C_{co}, wt%	C_{ao}, wt%	C_{at}, wt%	V_m, mV	$J_D\times10^8$, mol/cm^2 s [in absence of current]	$J_\theta\times10^8$, mol/cm^2 s [in absence of current]	$J_D\times10^8$, mol/cm^2 s [based on avg. data, in presence of current]	$J_\theta\times10^8$, mol/cm^2 s [based on avg. data, in presence of current]	$J_p\times10^8$, mol/cm^2 s	$J_m\times10^8$, mol/cm^2 s	SSD
1	30.3	1.13	1.13	2.26	0.000	0.000	0.000	−0.372	−0.129	32.585	--	--
2	30.3	2.26	1.13	2.89	−8.899	0.525	0.008	−0.213	−0.128	8.459	9.223	0.587
3	30.3	4.45	1.17	3.36	−17.152	1.523	0.031	0.765	1.197	10.525	8.845	0.460
4	30.3	3.93	1.11	3.2	−15.556	1.281	0.025	0.525	0.952	9.543	9.727	0.033
5	30.3	2.26	3.39	4.61	5.206	−0.525	−0.005	−1.100	−0.648	5.863	6.965	0.038
6	20.2	4.43	1.08	2.57	−18.122	1.555	0.033	0.882	1.353	7.161	6.983	0.103
7	20.2	4.52	5.88	7.4	3.377	−0.631	−0.006	−1.075	−0.840	7.305	6.983	0.103
8	20.2	3.91	1.11	2.32	−16.167	1.300	0.026	0.554	0.829	6.810	6.856	0.002
9	20.2	2.26	3.36	4.65	5.092	−0.511	−0.005	−1.106	−0.645	5.163	--	--
10	20.2	2.26	3.41	4.68	5.281	−0.534	−0.005	−1.085	−0.637	5.086	--	--
11	20.2	2.35	1.02	2.4	−10.716	0.617	0.010	−0.069	0.023	6.632	6.384	0.061
12	20.2	1.15	1.15	2.29	0.000	0.000	0.000	−0.755	−0.135	15.990	--	--
13	10.1	2.26	0.97	1.67	−10.860	0.599	0.010	0.242	0.318	3.364	3.297	0.004
14	10.1	1.13	1.13	2.29	0.000	0.000	0.000	−0.217	−0.158	2.739	--	--
15	10.1	4.43	1.11	1.86	−17.770	1.541	0.032	1.163	1.851	3.605	3.915	0.097
16	10.1	3.93	1.92	2.82	−9.197	0.933	0.015	0.611	0.773	3.806	0.233	0.001
17	4.0	2.28	1.11	1.52	−9.242	0.543	0.009	0.373	0.479	1.642	1.301	0.116
18	4.0	3.73	3.34	3.77	−1.418	0.181	0.002	0.065	0.067	1.722	1.755	0.001
19	4.0	4.43	1.11	1.4	−17.770	1.541	0.032	1.359	2.350	1.760	1.5174	0.0589
20	2.1	3.07	1.11	1.34	−13.061	0.910	0.016	0.781	1.165	0.921	0.891	0.001
21	2.1	2.28	1.11	1.33	−9.242	0.543	0.009	0.429	0.563	0.901	0.616	0.081
22	2.0	4.31	1.11	1.35	−17.417	1.486	0.030	1.370	2.380	0.901	0.9010	0.0000

yte and anolyte concentration difference, respectively. Flux could be positive or negative depending on ionic movements from catholyte to anolyte or the vice versa based on V_m generated as well as concentration gradient. In the present study, all the practical flux values were positive as the ionic movement was from catholyte to anolyte, implying that there was a definite effect of applied current on flux, as a result of which, ions could move against the concentration gradient. It was even observed that the flux had increased with applied current as well as initial concentration, with minor effect of anolyte concentration. This shows that when applied voltage and current values are very high for such type of dilute solution system, flux is influenced mainly by initial concentration, applied voltage and current only. However, the influence of anolyte concentration was observed to be marginal barring a few special cases where V_m was zero. Table 1 also includes the flux values calculated based on model equation (Eq. (18)) developed. We attempted to develop an equation to predict the practical molar fluxes. The proposed equation is applicable to the system where catholyte to anolyte initial concentration difference is positive. The values of the constant and the coefficients of Eq. (18), were calculated for positive initial concentration. Value of constant A was found to be 0.064, while the values of other coefficients such as a, b, c and d were calculated to be 0.285, 0.988, 0.009 and 2.397 respectively. Model based calculated flux values were compared with practical flux, and they were almost matching with minor deviations as shown in Fig. 3. Standard square deviation was also estimated as shown in Table 1. The proposed equation can be used when $C_{co}\neq C_{ao}$. Diffusion flux was neglected in this calculation as its effect was sup-

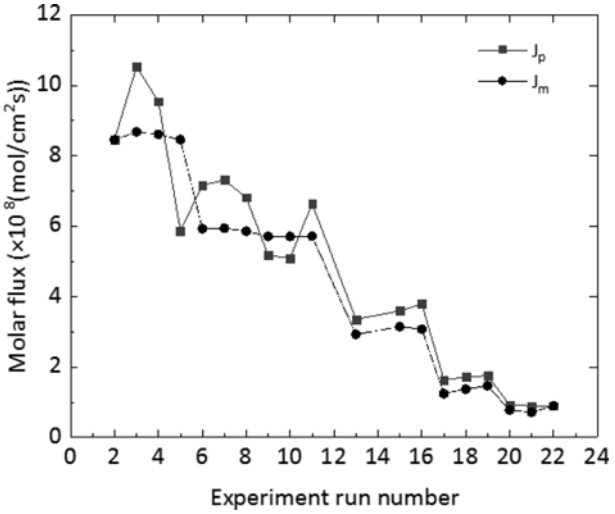

Fig. 3. Variation between practical molar flux and flux calculated using model equation.

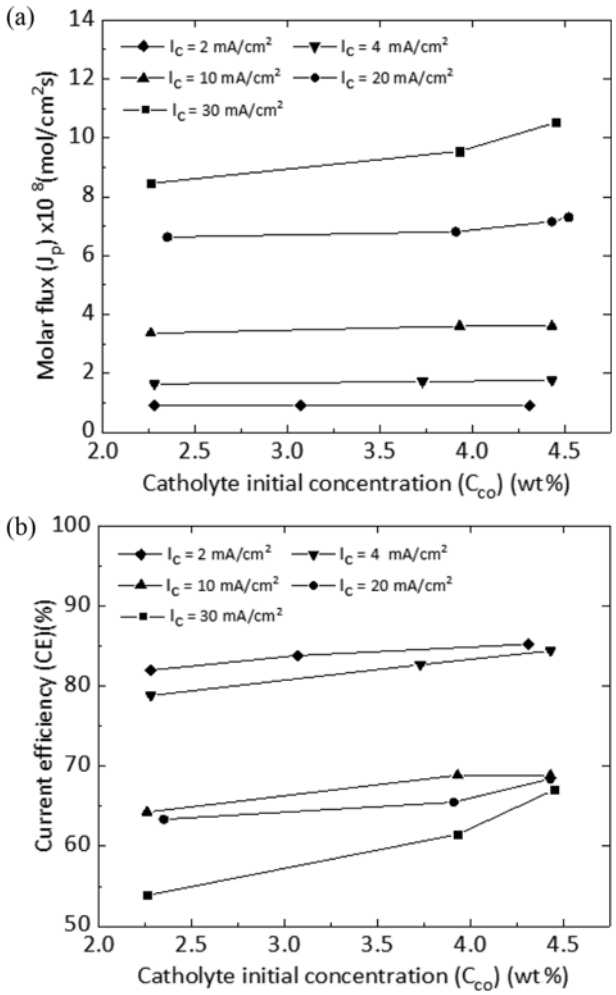

Fig. 4. Effect of catholyte initial concentration on (a) molar flux, (b) current efficiency at different constant current density.

posed to be very much less in the presence of higher applied current.

2. Effect of Initial Catholyte Concentration on Molar Flux and Current Efficiency

Initial catholyte concentration (C_{co}), can affect significantly the performance of the ED process. It affects molar flux, as ionic mobility and diffusive flux are functions of initial catholyte concentration. Effect of initial catholyte concentration on molar flux at constant current density is presented in Fig. 4(a). It shows that the flux increased almost linearly with initial catholyte concentration for current densities 10 mA cm^{-2} and above; however, for lower current densities there was negligible enhancement. For current density of 10 mA cm^{-2}, the maximum increase of molar flux with increasing catholyte concentration was estimated to be 3.6×10^{-8} mol cm^{-2} s^{-1}, whereas for current density of 20 mA cm^{-2} and 30 mA cm^{-2} maximum increase of molar fluxes were 7.15×10^{-8} mol cm^{-2} s^{-1} and 10.5×10^{-8} mol cm^{-2} s^{-1}, respectively. At very much lower values of current density, 2 and 4 mA cm^{-2}, marginal change was observed. As concentration of ions increases in the solution, it essentially provides the driving force to the movement of ions, and as a consequence molar flux increases. The greater the number of ions present in the solution, the higher becomes the flux obtained. However, in the present work, experiments were conducted in a lower range of initial concentration range up to 5 wt% only. Thus, it may not be appropriate to assign any optimal initial catholyte concentration value or range. For that, more experiments are required to be performed at higher initial concentration. Nevertheless, on the basis of present experimental work, 4.45 wt% could be considered as most suitable initial catholyte concentration for which higher molar flux was obtained.

Fig. 4(b) presents the variation of current efficiency with respect to initial catholyte concentration at constant applied current density. An increasing trend was observed with increase in initial catholyte concentration in the present work. But beyond certain range of initial catholyte concentration, the system might have reached a maximum current efficiency and then decreased to lower values [26].

Fig. 4(b) indicates that for applied current densities 10, 20 and 30 mA cm^{-2}, the values of current efficiency increased from 64.27 to 68.86%, 63.35 to 69.78% and 53.86 to 67.02%, respectively, when initial catholyte concentration increased in the range from almost 2.2 to 4.5 wt%. Even at low current densities, such as 2 and 4 mA cm^{-2}, current efficiency increased. Furthermore, the current efficiencies were observed to be 78.8 to 85.23% at lower I_c, e.g., 2 to 4 mA cm^{-2}. However, current efficiency decreased when I_c increased from 10 to 30 mA cm^{-2} and was found to be in the range of 50 to 70% only. Similar observations were reported by Luo et al. [26] in the process of concentration of formic acid solution by electrodialysis. Note that the solution conductivity as well as current efficiency increase with increasing solution concentration till the values reach maximum current efficiency [26,27]. This underscores the importance of performing more experiments at higher concentration. Therefore, the determination of maximum current efficiency assumes significance, which unfortunately could not be carried out in the present experimental conditions as the feed solution was very dilute, having low concentrations of sulfuric acid.

3. Effect of Applied Current Density on Molar Flux and Current Efficiency

The molar flux through ion exchange membrane depends upon the current flowing between anode and cathode. Experiments were performed to observe the behavior of the process for different applied electric current densities. Fig. 5(a) presents the molar flux as a function of applied current density for three different catholyte concentrations: 2.26, 3.9 and 4.3 wt%. Molar flux was found to increase almost linearly with applied current densities. It increased from 0.9×10^{-8} to 6.63×10^{-8}, 0.92×10^{-8} to 9.54×10^{-8} and 0.84×10^{-8} to 10.52×10^{-8} mol cm^{-2} s^{-1} for given values of catholyte initial concentrations when current density varied from 2 to 30 mA cm^{-2}. Maximum flux was obtained at a current density 30 mA cm^{-2} and at 4.45 wt% initial catholyte concentration. Fundamentally, the function of applied current density is to push the anions towards the anode. Higher the applied current density, the higher will be the applied force, resulting in enhanced flux. At higher current density, less time is required by the system to transport ions from catholyte to anolyte, and higher flux is achieved. If the time required to transport the same number of ions from cathode to anode at higher current density is less, the process becomes faster. The data pre-

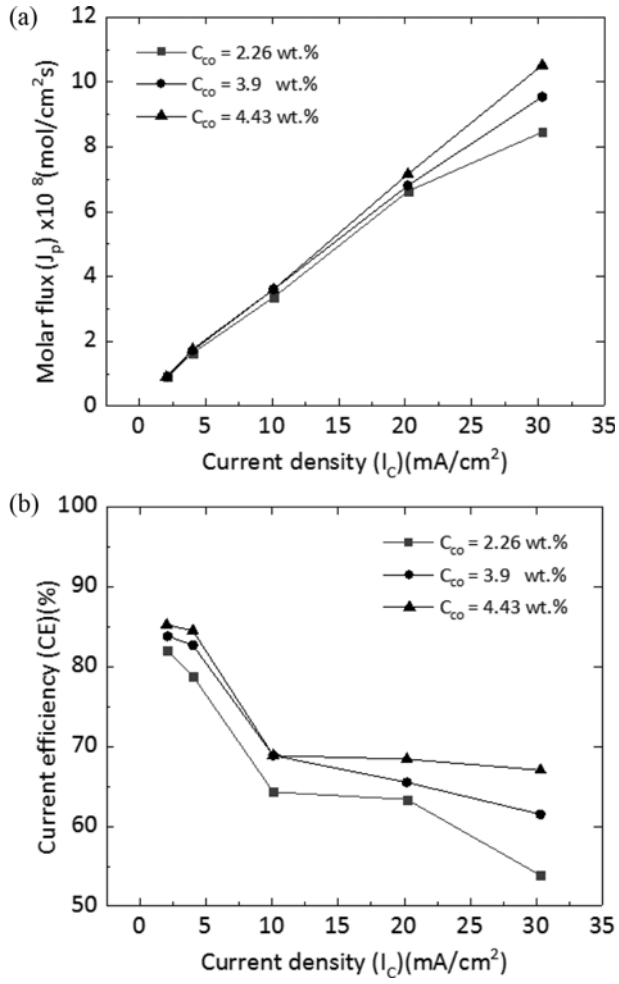

Fig. 5. Effect of current density on (a) molar flux, (b) current efficiency at different constant catholyte initial concentration.

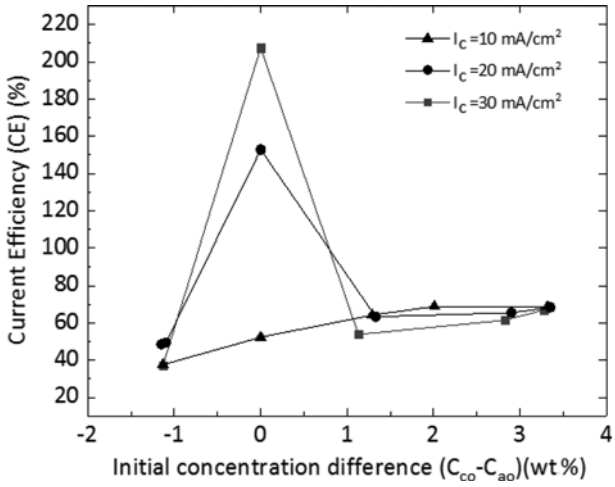

Fig. 6. Effect of catholyte and anolyte initial concentration difference on current efficiency.

sented in Fig. 5(a) reveal that the rate of change of flux was more affected by applied current density than by initial catholyte concentrations. From Fig. 5(b) it is clear that current efficiency decreased with current density at constant initial catholyte concentration (C_{co}). The present system was so dilute that current efficiency was found to decrease beyond applied current density 2 mA cm^{-2}, presumably due to the onset of limiting current density, water splitting at the membrane surface as well as higher electrical resistance [26,28]. Thus, current efficiency was found to decrease with applied current density for constant initial catholye concentration [28]. When C_{co} was 2.26 wt%, efficiency decreased from 81.9 to 53.8%, and for C_{co} 3.9 wt% it decreased from 83.8 to 61.4%.

At constant composition, the current efficiency was higher at lower applied current densities [26,28]. When I_c was kept in the range 2 to 4 mA cm^{-2}, efficiencies were estimated to be in the range of 78.8 to 85.23%. This was plausibly due to the mobility and current carrying capacity of the ions. Initially, at lower I_c no negative effects such as volume change and water splitting at the electrode were observed. As a result, the current efficiency was higher in all cases at lower I_c. As separation proceeded, catholyte became dilute with concentration becoming less than the initial concentration, thereby reducing the number of ions in the solution. This might have led to reduced utilization of the actual current supplied. As I_c increased further, bubble formation on the surface of membrane took place, with little change in volume as well as temperature of the solution. The bubbles were due to the formation of hydrogen gas at the cathode, and as a result the movement of ions from catholyte to anolyte decreased. Applied current density is not a certain value [26] and it can change with the working system and the properties of the membranes. Best results were observed for lower I_c and higher initial catholyte concentrations for the present process.

Higher efficiencies were obtained at lower current density values 2 to 4 mA cm^{-2} but at higher initial catholyte concentration of 4.45 wt% and with minimum molar flux. So, for the present process, 20 to 30 mA cm^{-2} current density can be suggested as the appropriate range where molar flux is also reasonably higher and efficiencies are in the range 60 to 70%. Taken together these observations point out that the ED used in the work was a less energy-intensive process for separation of sulfuric acid from its solution.

4. Effect of Catholyte and Anolyte Initial Concentration Difference

The effect of initial concentration difference of catholyte and anolyte on the current efficiency (CE) is presented in Fig. 6. Perusal of Fig. 6 implies that when the process was operated using equal catholyte and anolyte initial concentration (C_{co}=C_{ao}), the CE were reported to be very high, even more than 100% for some cases [26]. When the values of applied current density were 20 and 30 mA cm^{-2}, CE was estimated to be 152.7% and 207.5% respectively. Due to similar anolyte and catholyte initial concentrations at the beginning of the process, no membrane potential gradient could be generated. In such case in absence of current and diffusive resistances offered by solution as well as membrane were same on both the sides. This could be the reason for obtaining maximum CE as well as flux for this case. Even for the studied dilute solution with catholyte initial concentration about 1±0.1 wt%, when experiments were performed at higher applied current density, 20 and 30 mA cm^{-2}, it was observed that the movement of ions was very fast. Al-

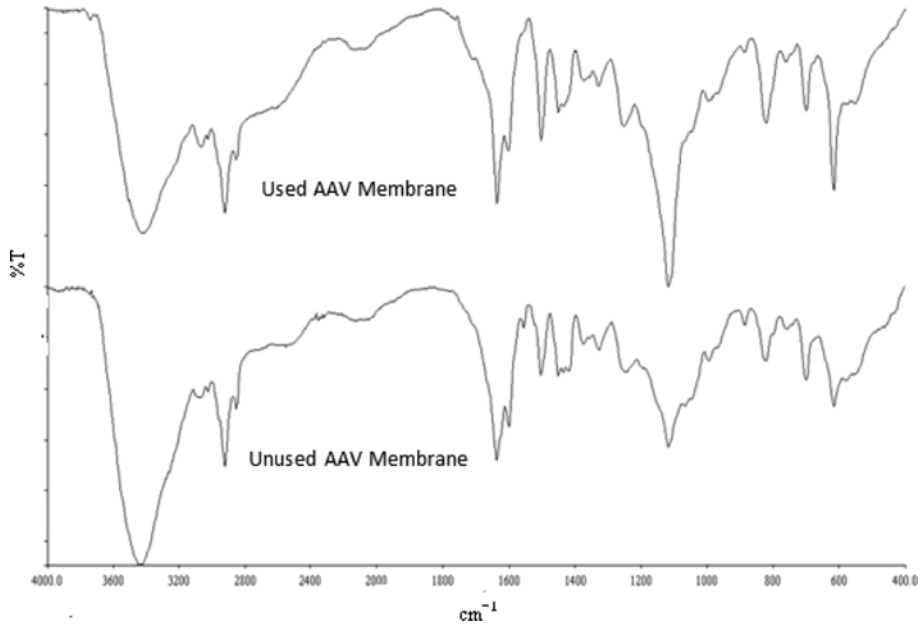

Fig. 7. FTIR spectra of AAV membrane used in present study.

Table 2. Principal band assignments of FTIR spectra over wave number 4,000-400 cm^{-1}

Wave numbers (cm^{-1})	Band assignment
3025.78; 3071.83	C=C stretching vibration
1452.62; 1436.01	Skeletal in plane stretching vibration C=C
2925-2854	Stretching vibration of -CH_2 group
1328.76; 968.07	Bending vibration of CH_3 group in aliphatic chain
3441	Stretching vibration of O-H
1117.48	Stretching vibration of C-N vibration of quaternary ammonium group
1068	C-H bending vibration

though maximum molar flux was obtained, the experiment could not be carried out for longer time. CE suddenly dropped thereafter but once again gradually increased for positive concentration difference. When experiments were carried out after maintaining positive catholyte to anolyte initial concentration difference (C_{co}> C_{ao}), CE was found to increase for almost all cases. This has already been discussed in section 3.2 in detail. If special case (C_{co}=C_{ao}) data were to be ignored, overall it was found to be an increasing trend of CE for C_{co}>C_{ao}. Reverse trend was observed for negative catholyte to anolyte initial concentration difference (C_{co}<C_{ao}). CE was reported to be 37.3%, 49.3% and 37.6% for current densities of 30, 20 and 10 mA cm^{-2} respectively. CE with negative concentration difference was even less than that with positive concentration difference. When anolyte concentration was more than catholyte concentration, efficiencies were found to be very less. This proves that there is a definite effect of anolyte initial concentration on current efficiency. When catholyte initial concentration was increased, CE increased as well, but it subsequently decreased with increase in anolyte initial concentration. This may be due to back diffusion of ions from anolyte to catholyte restricting the movement of ions in the opposite direction of concentration gradient, i.e., from catholyte to anolyte, and ultimately it requires more applied current to move and hence lesser CE. These observations are in good agreement with those reported by Luo et al. [26] in the electrodialysis of formic acid solution.

5. FTIR Analysis

Interpretation of the FTIR spectrum can be of great help in determining the presence of functional groups in the ion-exchange membrane specimen. A close inspection of the FTIR spectra of the pristine and used membranes as presented in Fig. 7 indicates the presence of a number of sharp, medium and broad peaks in the entire range of 400-4,000 cm^{-1}. Principal band assignments of FTIR spectra over wave number 4,000-400 cm^{-1} are presented in Table 2. The AAV ion exchange membrane is fabricated by copolymerization of styrene, chloromethyl styrene and divinyl-benzene followed by subsequent incorporation of quaternary ammonium group as ion-exchange functional group. The peaks at 3,025.78 cm^{-1} and 3,071.83 cm^{-1} are associated with the stretching vibration of C=C groups of aromatic hydrocarbons, which corroborates the grafting of styrene in the anion exchange membrane [29]. Two distinctly characteristic broad absorption bands, one at 3,441 cm^{-1} and the other at 1,117.48 cm^{-1}, represent the stretching vibration of O-H of water molecules and C-N bond of quaternary ammonium group, respectively. The observations indicate that quater-

nary ammonium group has been adequately incorporated into the AAV anion exchange membrane. The couple of bands at 701.45 and 761.12 cm^{-1} can be ascribed to the aromatic C-H deformation of mono-substituted benzene ring of grafted polystyrene of the AAV membrane. The band at 825 cm^{-1} is due to di-substituted benzene ring of divinyl benzene cross link of the membrane. It was observed from the spectral analysis that due to quaternization the IR bands of aromatic ring C=C and aromatic ring backbone -CH- bending vibration were shifted to relatively lower frequencies. Broadening and shifting of certain bands might have occurred as a result of quaternization and copolymerization reaction and introduction of ion exchange groups, thereby making them inadequate for precise quantitative determinations [30]. Additionally, a lower wave number represents the increase in the bond length, and this might be a result of the electrostatic interaction between the functional groups present in the anion exchange membrane.

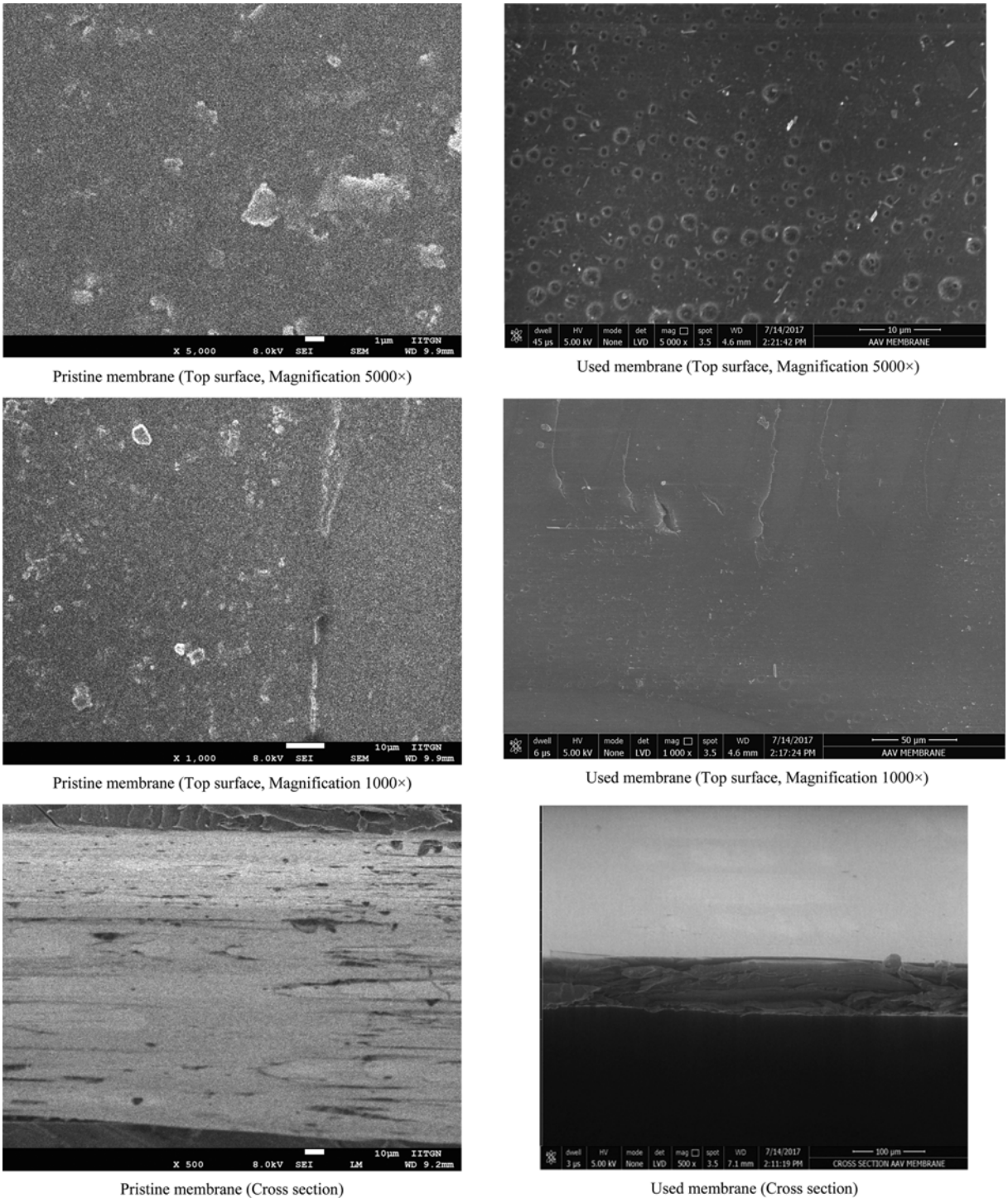

Fig. 8. SEM micrographs of cross section and top surface of AAV membrane under different magnifications used in present study.

6. Surface Topography by SEM Analysis

The surface topography of the pristine and used AAV membrane from the present study of electrodialysis of dilute sulfuric acid was investigated following scanning electron microscopy (SEM). Fig. 8 represents the SEM micrograms of the membrane specimens at two different magnifications. The microgram of the pristine membrane suggests the appearance of a compact and smooth surface without much visible pores. The absence of any surface irregularities or cracks signifies homogeneity and compactness of membrane. This probably confirms good compatibility between ion exchange functional group and the polymer matrix. The cross-section of the anion exchange membranes was also found to be densely porous and compact, facilitating the electrodialysis process. It is assumed that the pores generate easy flow channels for the counter-ion transportation. A few white smudges on the top surface of the pristine membrane were probably due to the improper adjustment of the scan. The scan pattern might have become nonlinear, particularly at the edges of the image at high magnifications. On the other hand, a perusal of the top surface of the used membrane reveals that the pores were shrouded with a slim layer, as a result of ionic transport experienced by the AAV membrane. With higher magnification (5000) the clusters were also visible almost on the entire surface. Moreover, there was a slight difference in pore morphology in the regions close to outer surface as compared to the rest of the membrane. The appearance of pleat and cluster on the edges of the outer surface of the used membranes could be due to dehydration and shrinkage of the polymer. Taken together, the observations from the SEM analysis suggest that the skin layer of the pristine membranes had a homogeneous morphology suitable for the transport of ions during the electrodialysis process. The AAV membrane was able to deliver favorable ionic conducting performance with improved electrochemical characteristics. However, the impact on the polarization phenomenon could not be ascertained under present experimental setup.

CONCLUSIONS

The present study demonstrates that electrodialysis can be effectively used for the separation and concentration of sulfuric acid from its dilute solution. Applied current density and initial catholyte concentration have profound influence on molar flux as well as current efficiency. Flux increased almost linearly with initial catholyte concentration for current densities of 10 mA cm^{-2} and above; however, for lower current densities there was negligible enhancement. The maximum molar flux was estimated to be 10.52×10^{-8} mol cm^{-2} s^{-1} at 4.45 wt% initial catholyte concentration and 30 mA cm^{-2} applied current density. Current efficiencies were observed to be 78 to 85% at lower current densities, which rose to more than 100% at 20 and 30 mA cm^{-2}, for the same catholyte and anolyte initial concentration. The contribution of diffusive flux as well as membrane potential based flux calculated either in presence or absence of current was very less as against practical flux obtained in presence of applied electric current. The molar flux was predominantly due to the influence of the applied electric field. An equation was developed to predict the molar fluxes which matched satisfactorily with experimental values with minor standard square deviations. FTIR spectra of the membrane specimen indicated broadening and shifting of certain bands as a result of quaternization and copolymerization reaction and introduction of ion exchange groups. The SEM analysis suggests that the skin layer of the pristine membrane had a homogeneous morphology, rendering it amenable for delivering favorable ionic conducting performance with the present system. The data obtained in the present study would be useful as guidelines for scale up of electrodialysis; nevertheless, the effects of back diffusion and concentration polarization constitute important areas of future research towards its commercialization.

ACKNOWLEDGEMENTS

The authors are grateful to Sophisticated Instrumentation Centre for Advance Research & Testing (SICART), Vallabh Vidyanagar and Indian Institute of Technology, Gandhinagar for their valuable support to carry out certain analyses. Suggestions by the anonymous reviewers to improve the manuscript are also gratefully acknowledged.

NOMENCLATURE

A : membrane surface area [cm^2]
C_{co} : catholyte initial concentration [wt%]
C_{ao} : anolyte initial concentration [wt%]
C_{ct} : catholyte concentration with time [wt%]
C_{at} : anolyte concentration with time [wt%]
C_{cf} : catholyte final concentration [wt%]
C_{af} : anolyte final concentration [wt%]
CE : current Efficiency
dC_t : anolyte to catholyte concentration difference (C_{at}-C_{ct}) [wt%]
dC_c : catholyte concentration variation with time (C_{ct}-C_{co}) [wt%]
F : faraday constant
J_u : flux due to motion/velocity of fluids
J_D : flux due to natural diffusion based on concentration gradient
$J_{Ø}$: flux due to migration of ions based on membrane electric potential developed due to concentration difference
$J_{Øa}$: flux due to applied electric potential
J_p : flux calculated practically based on experimental data
J_m : flux predicted based on model equation developed
I_c : applied current density [mA/cm^2]
m : mobility of ions in solution
R : absolute gas constant
T : temperature [K]
t : time [min]
V_l : volume of solution [ml]
V_m : membrane potential based on concentration difference across the membrane
x : membrane thickness, 112 μm
z : valence number of ions
μ : viscosity of acidic solution
Ø : electrical potential

REFERENCES

1. A. Agrawal and K. K. Sahu, *J. Hazard. Mater.*, **171**, 61 (2009).

2. A. Lopez-Delgado, F. J. Alguacil and F. A. Lopez, *Hydrometallurgy*, **45**, 97 (1997).
3. T. Ozdemir, C. Oztin and N. S. Kıncal, *Chem. Eng. Comm*., **193**, 548 (2006).
4. U. Kerney, *Resour. Conserv. Recycl*., **10**, 145 (1994).
5. V. Nenov, N. Dimitrova and I. Dobrevsky, *Hydrometallurgy*, **44**, 43 (1997).
6. R. M. Hudson, ASM International, Material Park, Ohio, *ASM Handbook*, **3**, 67 (1994).
7. U. K. Kesieme, H. Aral, M. Duke, N. Milne and C. G. Cheng, *Hydrometallurgy*, **138**, 14 (2013).
8. K. Nath, *Membrane separation processes*, PHI, New Delhi, 233 (2017).
9. M. A. S. Rodrigues, A. M. Bernardes and J. Z. Ferreira, Conference: EPD Congress, Minerals, Metals and Materials Society/AIME, 184 Thorn Hill Road, Warrendale, PA 15086-7528, USA:659-672 (1999).
10. L. Cifuentes, G. Crisostomo, J. P. Ibanez, J. M. Casas, F. Alvarez and G. Cifuentes, *J. Membr. Sci*., **207**, 1 (2002).
11. J. Winiewski, G. Wigniewska and T. Winnicki, *Desalination*, **169**, 11 (2004).
12. M. C. Martí-Calatayud, D. C. Buzzi, M. Garcia-Gabaldon, E. Ortega, A. M. Bernardes, J. A. S. Tenori and V. Perez-Herranz, *Desalination*, **343**, 120 (2014).
13. M. C. Martí-Calatayud, M. García-Gabaldon and V. Perez-Herranz, *J Membr. Sci*., **443**, 181 (2013).
14. D. C. Buzzi, L. S. Viegas, M. A. S. Rodrigues, A. M. Bernardes and J. A. S. Tenorio, *Miner. Eng*., **40**, 82 (2013).
15. H. Jaroszek, W. Mikołajczak, M. Nowak and B. Pisarska, *Desalination Water Treatment*, **64**, 223 (2017).
16. G. Pourcelly, I. Tugas and C. Gavach, *J. Membr. Sci*., **97**, 99 (1994).
17. A. T. Cherif, C. Gavach, T. Cohen, P. Dagard and L. Albert, *Hydrometallurgy*, **21**, 191 (1988).
18. K. Urano, T. Ase and Y. Naito, *Desalination*, **51**, 213 (1984).
19. A. T. Cherif and C. Gavach, *J. Electroanal. Chem*., **265**, 143 (1989).
20. S. Koter and M. Kultys, *J. Membr. Sci*., **318**, 467 (2008).
21. Y. Lorrain, G. Pourcelly and C. Gavach, *J. Membr. Sci*., **110**, 181 (1996).
22. Y. Lorrain, G. Pourcelly and C. Gavach, *Desalination*, **109**, 231 (1997).
23. D. J. Lewis and F. L. Tye, *J. Appl. Chem*., **9**, 279 (1959).
24. M. W. Verbrugge and R. F. Hill, *J. Electrochem. Soc*., **137**(4), 1131 (1990).
25. R. Audinosa, A. Nassr-allah, J. R. Alvarezb, J. L. Andresb and R. Alvarezb, *J. Membr. Sci*., **76**, 147 (1993).
26. G. S. Luo, S. Pan and J. G. Liu, *Desalination*, **150**, 227 (2002).
27. N. Kanavova and L. Machuca, *Periodica Polytechnica, Chem. Eng*., **58**(2), 25 (2014).
28. E. G. Akgemci, M. Ersoz and T. Atalay, *J. Sep. Sci. Technol*., **39**(1), 165 (2004).
29. M. M. Nasef and H. Saidi, *J. Membr. Sci*., **216**, 27 (2003).
30. M. Bartholin, *Makromol. Chem*., **182**, 2075 (1981).